J Mol Model (2003) 9:298–303
DOI 10.1007/s00894-003-0152-y

ORIGINAL PAPER

Venkatarajan S. Mathura · Kizhake V. Soman · Tushar K. Varma · Werner Braun

A multimeric model for murine anti-apoptotic protein Bcl-2 and structural insights for its regulation by post-translational modification

Received: 14 May 2003 / Accepted: 1 July 2003 / Published online: 30 August 2003

Abstract A monomeric model for murine antiapoptotic protein Bcl-2 was constructed by comparative modeling with the software suite MPACK (EXDIS/DIAMOD/FANTOM) using human Bcl-xL as a template. The monomeric model shows that murine Bcl-2 is an all α-helical protein with a central (helix 5) hydrophobic helix surrounded by amphipathic helices and an unstructured loop of 30 residues connecting helices 1 and 2. It has been previously shown that phosphorylation of Ser 70 located in this loop region regulates the anti-apoptotic activity of Bcl-2. Based on our current model, we propose that this phosphorylation may result in a conformational change that aids multimer formation. We constructed a model for the Bcl-2 homodimer based on the experimentally determined 3D structure of the Bcl-xL: Bad peptide complex. The model shows that it will require approximately a half turn in helix 2 to expose hydrophobic residues important for the formation of a multimer. Helices 5 and 6 of the monomeric subunit Bcl-2 have been proposed to form an ion-channel by associating with helices 5 and 6 of another monomeric subunit in the higher-order complex. In the multimeric model of Bcl-2, helices 5 and 6 of each subunit were placed distantly apart. From our model, we conclude that a global conformational change may be required to bring helices 5 and 6 together during ion-channel formation.

Keywords Homology modeling · Distance geometry · Apoptosis

V. S. Mathura · K. V. Soman · W. Braun (✉)
Sealy Center for Structural Biology, Dept. Human Biological Chemistry and Genetics,
University of Texas Medical Branch,
301 University Boulevard, Galveston, TX, 77555-1157, USA
e-mail: werner@newton.utmb.edu
Tel.: +1 409 747-6810
Fax: +1 409 747-6850

T. K. Varma
Educational Cancer Center, Department of Anesthesiology,
University of Texas Medical Branch,
Galveston, TX, 77555, USA

Present address:
K. V. Soman, The Bioinformatics Program,
University of Texas Medical Branch,
Galveston, TX, 77555, USA

Introduction

Programmed cell death (apoptosis) is a highly conserved process in the development of eukaryotic cells, leading to the removal of appropriate cells during development. Apoptosis also takes place in response to intracellular damage. [1] Dysregulation of apoptosis can lead to pathological states such as cancer by defective cell accumulation or neurodegeneration by cell loss. An understanding of the apoptotic machinery is therefore crucial for developing successful therapeutics of these diseases. [2]

Proteins that belong to the Bcl-2 family regulate the central death pathway and they are found in diverse members of eukaryotes. [1, 3, 4, 5, 6] The Bcl-2 family comprises several members with pro-apoptotic and anti-apoptotic functions, [7] and is characterized by four conserved domains referred to as Bcl-2 homology domains or BH domains. [3, 4, 8, 9] A delicate balance, essential for cellular homeostasis, exists between pro- and anti-apoptotic members in normal cells at physiological state. The exact homeostatic mechanism and apoptotic pathway constituted by Bcl-2 family members is not clear. Members of the Bcl-2 family are thought to function by forming homo- or hetero-dimers and tend to modulate the effect of opposite members within the family. [3, 4, 10, 11, 12, 13, 14, 15, 16, 17, 18, 19] For example Bcl-2, an anti-apoptotic member interacts and chelates Bax, a pro-apoptotic member, by forming a hetero-dimer that prevents Bax from associating with itself to form a killer ion-channel that disrupts the potential across the mitochondrial membrane. [12] Anti-apoptotic members also interact among themselves, which results in the formation of homodimers or homogeneous higher order complexes. [19] It is considered that such complexes form homeostatic ion-

channels that help to maintain the integrity of mitochondria during stress. [20, 21, 22, 23, 24, 25, 26, 27, 28] Dimerization by both Bcl-2/Bax and Bcl-2/Bcl-2 was inhibited by BH3 peptides derived from Bax and Bak, indicating that there is a common binding site that mediates Bcl-2 homodimerization and heterodimerization with Bax. [29] Structural studies by both X-ray crystallography and NMR spectroscopy have been reported for several Bcl-2 family members such as anti-apoptotic Bcl-xL, Bcl-2 and pro-apoptotic Bid and Bax. [17, 30, 31, 32] To date, the only available structural information about multimeric forms of the Bcl-2 family comprise the NMR structure of the heteromeric complex of Bcl-xL with a short peptide from Bak and Bad. [16, 17, 33, 34] The complete structure of a multimeric form of Bcl-2 is still unknown due to experimental difficulties in obtaining large quantities of soluble multimeric forms for X-ray and NMR structure determination. Theoretical methods like comparative modeling, [35] and docking techniques [36, 37, 38, 39] are alternative procedures for investigating the structural details of such complexes. We have used our modeling suite to construct homology models for human decay accelerating factor, [40] measles virus receptor CD46 [41] and pollen allergen Jun a 3. [42] Here we construct a 3D multimeric model of the murine anti-apoptotic protein Bcl-2 and relate its 3D structure to its regulatory function. In this paper, we describe our strategy for a flexible docking procedure in the construction of a Bcl-2 dimer using our distance geometry approach, [31, 43, 44] and present a detailed hypothesis for a conformational change of Bcl-2 in the transition from a monomeric to a dimeric form.

Methods

Template identification

Murine protein sequence (P10417) was obtained from the annotated protein database SWISSPROT. [45] A BLAST search with murine Bcl-2 as the query was performed in the PDB sequence database. [46] Human Bcl-2 (PDB code: 1GJH, 1G5M), human Bcl-xL(PDB code: 1LXL,1MAZ), rat Bcl-xL(PDB code:1AF3), human Bcl-xL-Bak peptide complex (PDB code:1BXL), and human Bcl-xL-Bad peptide complex (PDB code:1G5J) were identified with high scores ranging from 276 to 167 bits and all expectation values below 0.001. Bcl-2 and Bcl-xL are closely related proteins by function and have significant sequence identity of 47%. They also share all the Bcl-2 homology domains (BH1-BH4). The only information on dimeric structures is currently available from the two Bcl-xL peptide complexes. Since the structure of the Bcl-xL-Bad peptide complex is comprised of 25 residues bound to the dimerization groove of Bcl-xL with a binding affinity of Kd = 0.6 nM, which compares to 16 residues of Bak peptide in the structure of Bcl-xL:Bak peptide complex with a binding affinity of Kd = 480 nM, we used the Bcl-xL-Bad peptide complex to extract geometric constraints for the Bcl-2 dimeric model. [16] We rationalized that additional interactions observed in the Bcl-xL:Bad peptide compared to the Bcl-xL:Bak peptide will enable more precise docking of two Bcl-2 monomers to form a homodimer.

Sequence alignment for modeling

All sequence alignments were performed with the program CLUSTALW (version 1.8). [47] To construct a homodimer of Bcl-2, we identified a region in the Bcl-2 sequence that matches with the Bad peptide, as shown in Fig. 1a,b. All residues of Bcl-2 outside this peptide-matching region were modeled based on Bcl-xL. The co-ordinates for the Bcl-xL: Bad peptide complex were used to extract geometric constraints for the dimeric structure as follows:

Extraction of geometrical constraints and generating the final model

Distance and dihedral constraints were extracted from the Bcl-xL-Bad complex using our geometry extraction program EXDIS, [44] included in our modeling suite MPACK. Structurally conserved regions or the fragments in the alignment defined by excluding gaps were used for extracting constraints. In order to handle insertions and deletion in the target sequence, we relaxed the constraints at the start and end of the fragments along with the inserted residues by setting φ and ψ angles of the backbone at 180°. If the residue type between the target and the template agree in the alignment then we also extract dihedral angles (ζ angles) for the side chain or else set

a

```
BCL2_MOUSE      MAQAGRTGYDNREIVMKYIHYKLSQRGYEWDAGDADAAPLGAAPTPGIFSFQ--PESNPM 58
BCLX_HUMAN      MSQS------NRELVVDFLSYKLSQKGYSWSQFSDVEENRTEAPEGTESEMETPSAINGN 54
                *:*:      ***:*:.:: *****:**.*.   *.:     *.  * . :.     *

BCL2_MOUSE      PAVHREMAARTSPLRPLVATAGPALSPVPPCVHLTLRRAGDDFSRRYRRDFAEMSSQLHL 118
BCLX_HUMAN      PSWHLADSPAVNGATGHSSSLDAREVIPMAAVKQALREAGDEFELRYRRAFSDLTSQLHI 114
                *: *   :. ..      :: ..      ..*: :**.***:*. **** *::::****:

BCL2_MOUSE      TPFTARGRFATVVEELFRDGVNWGRIVAFFEFGGVMCVESVNREMSPLVDNIALWMTEYL 178
BCLX_HUMAN      TPGTAYQSFEQVVNELFRDGVNWGRIVAFFSFGGALCVESVDKEMQVLVSRIAAWMATYL 174
                ** **   *  **:****************.***.:*****::**. **..** **: **

BCL2_MOUSE      NRHLHTWIQDNGGWDAFVELYGPSMRP-LFDFSWLSLKTLLSLALVGACITLGAYLGHK 236
BCLX_HUMAN      NDHLEPWIQENGGWDTFVELYGNNAAAESRKGQERFNRWFLTGMTVAGVVLLGSLFSRK 233
                * **..***:*****:****** .  .    .   : : :*:   *.. : **: :.:*
```

b

```
BCL2_MOUSE      VPPCVHLTLRRAGDDFSRRYRR 107
BAD_            AAQRYGRELRRMSDEFVDSFKK 164
                ..      *** .*:*   :::
```

Fig. 1. a Pairwise alignment between murine Bcl-2 and human Bcl-xL. The sequences of murine Bcl-2 (P10417) and human Bcl-xL (Q07817) were obtained from the SWISSPROT database and aligned using CLUSTALW. The regions that were modeled are shown in *bold*. The highly disordered loop region that contains the phosphorylation site Ser 70 in Bcl-2 is shown in *italics* and the C-terminal anchor helix is *underlined*. **b** Alignment between the peptide part of BAD in the complex structure of Bcl-xL (1G5J) and corresponding region in murine Bcl-2

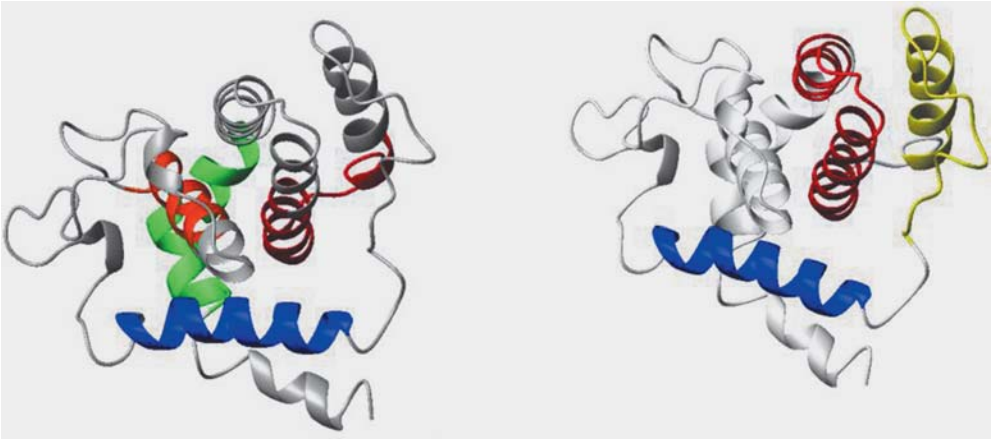

Fig. 2 Different Bcl-family homology domains (BH) and helices important for the formation of the dimerization domain. (*left*) BH1 domain (133–152) is shown in *red*, BH2 domain (184–199) in *green*, BH3 domain (90–104) in *blue*, BH4 domain (10–30) in *orange*. (*right*) Shown in *blue* is helix 2 (89–104), *yellow* is distorted helix 3 (111–118) and helix 4 (123–134), which forms the dimerization groove, helix 5 (140–160) and helix 6 (165–180) are shown in *red* and thought to form the ion-channel in a multimeric complex after insertion into a membrane

their values to 180°. Upper and lower distance constraints were fixed either by adding or subtracting a threshold of 0.5 Å to the actual distance. Similarly, 10° was added or subtracted to define the upper- and lower-bound dihedral angle constraints. A total of 15 distance constraints per atom were extracted from the matching regions of the template.

To direct the docking of one monomer of Bcl-2 into another, we extracted constraints from the Bcl-xL:Bad peptide by defining an axis for helix 2 of Bad at 1Å intervals. This corresponds to the axis of helix 2 of monomer B in the Bcl-2 dimer. Using our distance geometry program, we applied constraints between the monomer A (constraints obtained from Bcl-xL) and the monomer B (helix 2 constraints from the Bad peptide in the complex and the remaining residues from the Bcl-xL). Fifty models were generated starting from random conformations and the top ten models ranked according to increasing values of the target function were considered for visual analysis. The final model was energy minimized using the program FANTOM. [48] During the initial steps of constrained energy minimization, we used a fourth power energy penalty function and later on systematically reduced it to second power for violations above a threshold. The total conformational energy of the final model was negative. The geometry of the model was evaluated using PROCHECK. [49]

Results

Model for Bcl-2

Murine Bcl-2 is a 236-residue protein with a molecular weight of approximately 26 KDa. It has a long unstructured loop (residues 53–85), inferred by homology with Bcl-xL, with a phosphorylation site at Ser 70. This site is known to be important for the regulation of its anti-apoptotic activity. [50] The complete sequence of Bcl-2 also contains a 21-residue transmembrane region constituted by hydrophobic residues and considered to form a helix. This region anchors the cytoplasmic domain of Bcl-2. [51] The unstructured loop and the 21-residue C-terminal membrane anchor were not modeled due to the lack of a suitable template. The final model of murine Bcl-2 was highly similar to the human Bcl-2 structure with an RMSD of 1.0 Å. Murine Bcl-2 is an all-α-helical protein made up of seven helices with helix 5 completely buried (Fig. 2). Two monomers (A, B) of Bcl-2 dimerize in the hydrophobic pocket of monomer A, constituted by the BH3 and BH1 domains, with the helix 2 (BH3) of monomer B. In the monomeric form of Bcl-2, helix 2 consists of buried hydrophobic residues. In the dimer these hydrophobic residues were exposed as in the case of Bad/Bak peptides that interact with the hydrophobic groove of Bcl-xL. Helices 5 and 6 have structural similarity to ion-channel forming proteins like diphtheria toxin and Colicin. [23, 25, 26, 31] Previous studies have demonstrated that Bcl-2 forms a selective ion-channel. However, in our dimer model, these helices are located approximately 40 Å apart, indicating that an ion-channel might be composed of a higher order multimeric structure. This possibility is further supported by our model as the dimerization groove of one of the monomers and the helix 2 of the other monomer remain exposed, suggesting further potential interactions that lead to higher order multimerization.

Discussion

Conformational changes required for dimerization

The monomeric forms of human Bcl-2 and human Bcl-xL show that the hydrophobic residues in helix 2 (BH3 domain) are buried. In contrast, the hydrophobic residues in the Bak or Bad peptide that correspond to helix 2 of Bcl-2 are located on the monomeric surface in the Bcl-xL/peptide complex poised for interaction with the dimerization groove formed by helices 3, 4 and 5. A rigid body docking procedure utilizing the available human Bcl-2 monomer and these hydrophobic interactions for dimerization cannot be successful. Our initial attempts to satisfy

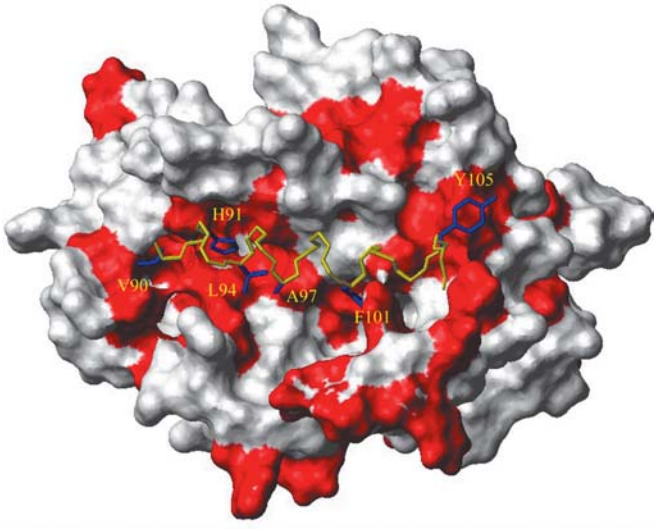

Fig. 3 Hydrophobic interactions in the dimerization groove are shown. Helix 2' of monomer B interacts through residues V90, H91, L94, A97, G98, F101, Y105 with the hydrophobic surface formed by residues in helices 3, 4, and 5 of the monomer A. Shown here is a lateral view of monomer A depicted in a surface model with hydrophobic regions in *red*. The backbone of helix is shown using neon representation in *yellow* and the interacting side chains are in *blue*

these hydrophobic interactions between helix 2 of one monomer and the dimerization groove of helices 3, 4 and 5 resulted in severe steric clashes (Fig. 3).

In the flexible docking procedure, we extracted constraints for residues outside the dimerization interface from the template structure and combined them with constraints of the interface as in the heteromeric complex of the Bcl-xL protein and peptide Bak. A 3D model consistent with these combined constraints is then calculated with our distance geometry approach. This resulted in a 3D dimeric model in which helix 2 (residues 90–104) underwent an approximately half turn rotation in order to expose hydrophobic residues buried in the corresponding monomeric forms of Bcl-2 (Fig. 4).

This conformational requirement may be induced by regulation at the upstream-unstructured loop due to phosphorylation at Ser 70 or by interaction with other proteins subsequent to phosphorylation. [50, 52] Phosphorylation at Asp 54 in the receiver domain of the bacterial enhancer-binding protein NtrC (nitrogen regulatory protein C) leads to an axial rotation of a helical segment and subsequent exposure of a hydrophobic surface that acts as a signal for transcriptional activation. [53, 54, 55] It has been shown for other members of the Bcl-2 family that the long unstructured loop is cleaved by caspases before the protein is activated. [56] If such a cleavage occurs in Bcl-2, it may reduce the strain while facilitating the possibility of helix 2 turning and forming a dimer.

Based on our model, we hypothesize that higher order multimers of Bcl-2 form homeostatic ion-channels, which apart from chelating pro-apoptotic members, play a critical role during stress. Under stress, some of the Bcl-2 proteins are activated and undergo conformational change in the helix 2 to form an ion-channel. At this stage it is also capable of chelating pro-apoptotic members. We base our hypothesis on the observation of Ito et al., who demonstrated that phosphorylation of Bcl-2 at Ser 70 results in increased anti-apoptotic activity of murine Bcl-2, critical for cell survival during stress. [50]

Dimeric model reveals higher order multimer possibility

It has been previously shown that the current conducted by the ion-channels formed by Bcl-xL stepped up with time and in electrophysiological studies Bcl-2, Bcl-xL forms higher ordered multimers (greater than 2) with increasing time. [22, 23, 25] Our observation from the model reveals that helix 2 of monomer A and helices of 3, 4 and 5 of monomer B are free to associate with other

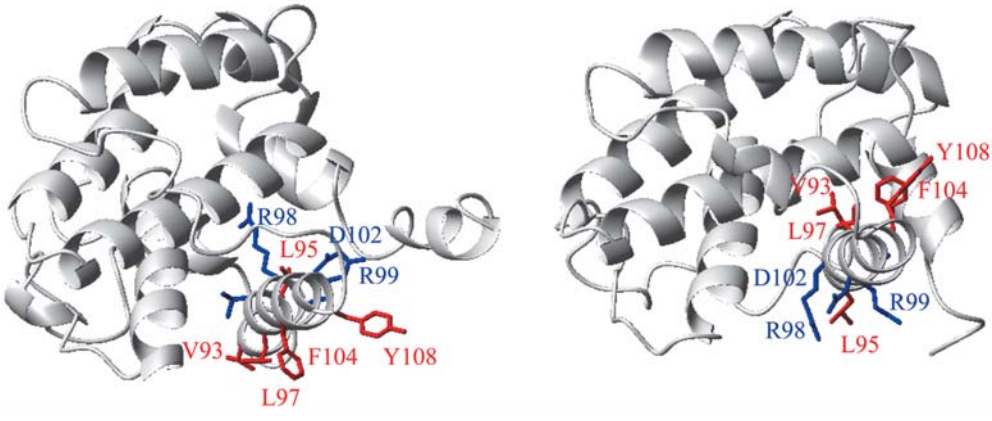

Fig. 4 Comparison of the murine Bcl2 model (*right*) and the structure of human Bcl-2 isomer (*left*) (PDB code:1G5M). The hydrophobic residues (V93, L97, F104, Y108) that are essential for multimer formation in the dimer model in helix 2 (residues 90–105) are exposed, whereas they are buried in the monomer structure. The residue numbers in murine Bcl-2 are shifted by +3 to match the human Bcl-2 numbering

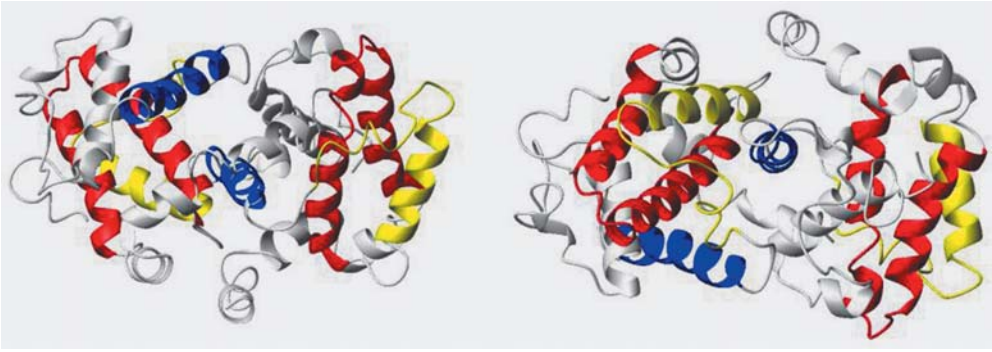

Fig. 5 Top (*left*) and bottom view (*right*) of murine Bcl-2 dimer model. Helices 5 and 6 that form the ion-channel are shown in *red*, helix 2 is shown in *blue*. Helices 3 (distorted) and helix 4 are shown in *yellow*. In monomer A the helices 3 and 4 form the dimerization groove into which helix 2' of monomer B fits. This model shows helix 2 of monomer A and helices 3', 4' monomer B are free to form higher order multimers

monomers progressively forming a higher ordered complex (Fig. 5). Preliminary attempts to generate a higher order closed complex suggest that it may take up to five monomers.

Conclusion

Our 3D model of the Bcl-2 dimer suggests a specific conformational change, a half-turn rotation of helix 2, in the monomer to dimer transition. We hypothesize that this conformational change may be facilitated by regulatory signals like phosphorylation and/or other regulatory proteins that bind to the loop region of Bcl-2 upon phosphorylation of Ser 70. Our model also suggests that higher order multimers of Bcl-2 can be formed when all constituting members have their hydrophobic amino acids in the helix 2 exposed to favor interaction with the hydrophobic groove of another monomer. Our current method can also be applied to constructing homodimers and heteromers among pro- and anti-apoptotic members of Bcl-2.

Acknowledgment We thank Dr. Stratford May at the Shands Cancer Center, University of Florida for suggestion of the problem and necessary guidance. We thank Dr. Aaron Domina, UTMB for his valuable comments. This project was supported in part by an ARP grant (004952-0084-1999) of the Texas Higher Education Coordinating Board and a grant from the Department of Energy (DE-FG03-00ER63041) to WB.

References

1. Korsmeyer SJ (1999) Harvey Lect 95:21–41
2. Kaufmann SH, Earnshaw WC (2000) Exp Cell Res 256:42–49
3. Adams JM, Cory S (1998) Science 281:1322–1326
4. Adams JM, Cory S (2001) Trends Biochem Sci 26:61–66
5. Chao DT, Korsmeyer SJ (1998) Annu Rev Immunol 16:395–419
6. Korsmeyer SJ (1993) Important Adv Oncol 19–28
7. Korsmeyer SJ (1999) Cancer Res 59:1693s–1700s
8. Gross A, McDonnell JM, Korsmeyer SJ (1999) Genes Dev 13:1899–1911
9. Gross A (2001) IUBMB Life 52:231–236
10. Gross A, Jockel J, Wei MC, Korsmeyer SJ (1998) EMBO J 17:3878–3885.
11. Korsmeyer SJ, Shutter JR, Veis DJ, Merry DE, Oltvai ZN (1993) Semin Cancer Biol 4:327–332
12. Cheng EH, Wei MC, Weiler S, Flavell RA, Mak TW, Lindsten T, Korsmeyer SJ (2001) Mol Cell 8:705–711
13. Korsmeyer SJ, Wei MC, Saito M, Weiler S, Oh KJ, Schlesinger PH (2000) Cell Death Differ 7:1166–1173
14. Lindsten T, Ross AJ, King A, Zong WX, Rathmell JC, Shiels HA, Ulrich E, Waymire KG, Mahar P, Frauwirth K, Chen Y, Wei M, Eng VM, Adelman DM, Simon MC, Ma A, Golden JA, Evan G, Korsmeyer SJ, MacGregor GR, Thompson CB (2000) Mol Cell 6:1389–1399
15. Oltvai ZN, Milliman CL, Korsmeyer SJ (1993) Cell 74:609–619
16. Petros AM, Nettesheim DG, Wang Y, Olejniczak ET, Meadows RP, Mack J, Swift K, Matayoshi ED, Zhang H, Thompson CB, Fesik SW (2000) Protein Sci 9:2528–2534
17. Sattler M, Liang H, Nettesheim D, Meadows RP, Harlan JE, Eberstadt M, Yoon HS, Shuker SB, Chang BS, Minn AJ, Thompson CB, Fesik SW (1997) Science 275:983–986
18. Yin XM, Oltvai ZN, Korsmeyer SJ (1995) Curr Top Microbiol Immunol 194:331–338
19. Sato T, Hanada M, Bodrug S, Irie S, Iwama N, Boise LH, Thompson CB, Golemis E, Fong L, Wang HG, Reed JC (1994) Proc Natl Acad Sci USA 91:9238–9242
20. Xie Z, Schendel S, Matsuyama S, Reed JC (1998) Biochemistry 37:6410–6418
21. Schendel SL, Reed JC (2000) Methods Enzymol 322:274–282
22. Schendel SL, Azimov R, Pawlowski K, Godzik A, Kagan BL, Reed JC (1999) J Biol Chem 274:21932–21936
23. Schendel SL, Montal M, Reed JC (1998) Cell Death Differ 5:372–380
24. Matsuyama S, Schendel SL, Xie Z, Reed JC (1998) J Biol Chem 273:30995–31001
25. Schendel SL, Xie Z, Montal MO, Matsuyama S, Montal M, Reed JC (1997) Proc Natl Acad Sci USA 94:5113–5118
26. Schlesinger PH, Gross A, Yin XM, Yamamoto K, Saito M, Waksman G, Korsmeyer SJ (1997) Proc Natl Acad Sci USA 94:11357–11362
27. Minn AJ, Velez P, Schendel SL, Liang H, Muchmore SW, Fesik SW, Fill M, Thompson CB (1997) Nature 385:353–357
28. Minn AJ, Kettlun CS, Liang H, Kelekar A, Vander Heiden MG, Chang BS, Fesik SW, Fill M, Thompson CB (1999) EMBO J 18:632–643
29. Diaz JL, Oltersdorf T, Horne W, McConnell M, Wilson G, Weeks S, Garcia T, Fritz LC (1997) J Biol Chem 272:11350–11355
30. McDonnell JM, Fushman D, Milliman CL, Korsmeyer SJ, Cowburn D (1999) Cell 96:625–634

31. Muchmore SW, Sattler M, Liang H, Meadows RP, Harlan JE, Yoon HS, Nettesheim D, Chang BS, Thompson CB, Wong SL, Ng SL, Fesik SW (1996) Nature 381:335–341
32. Ruffolo SC, Breckenridge DG, Nguyen M, Goping IS, Gross A, Korsmeyer SJ, Li H, Yuan J, Shore GC (2000) Cell Death Differ 7:1101–1108
33. Aritomi M, Kunishima N, Inohara N, Ishibashi Y, Ohta S, Morikawa K (1997) J Biol Chem 272:27886–27892
34. Petros AM, Medek A, Nettesheim DG, Kim DH, Yoon HS, Swift K, Matayoshi ED, Oltersdorf T, Fesik SW (2001) Proc Natl Acad Sci USA 98:3012–3017
35. Marti-Renom MA, Stuart AC, Fiser A, Sanchez R, Melo F, Sali A (2000) Annu Rev Biophys Biomol Struct 29:291–325
36. Fahmy A,Wagner G (2002) J Am Chem Soc 124:1241–1250
37. Smith GR, Sternberg MJ (2002) Curr Opin Struct Biol 12:28–35
38. Sternberg MJ, Gabb HA, Jackson RM (1998) Curr Opin Struct Biol 8:250–256
39. Strynadka NC, Eisenstein M, Katchalski-Katzir E, Shoichet BK, Kuntz ID, Abagyan R, Totrov M, Janin J, Cherfils J, Zimmerman F, Olson A, Duncan B, Rao M, Jackson R, Sternberg M, James MN (1996) Nat Struct Biol 3:233–239
40. Hasan RJ, Pawelczyk E, Urvil PT, Venkatarajan MS, Goluszko P, Kur J, Selvarangan R, Nowicki S, Braun WA, Nowicki BJ (2002) Infect Immun 70:4485–4493
41. Mumenthaler C, Schneider U, Buchholz CJ, Koller D, Braun W, Cattaneo R (1997) Protein Sci 6:588–597
42. Soman KV, Midoro-Horiuti T, Ferreon JC, Goldblum RM, Brooks EG, Kurosky A, Braun W, Schein CH (2000) Biophys J 79:1601–1609
43. Friesen RH, Castellani RJ, Lee JC, Braun W (1998) Biochemistry 37:15266–15276
44. Soman KV, Schein CH, Zhu H, Braun W (2001) Methods Mol Biol 160:263–286
45. O'Donovan C, Martin MJ, Gattiker A, Gasteiger E, Bairoch A, Apweiler R (2002) Brief Bioinform 3:275–284
46. Altschul SF, Madden TL, Schaffer AA, Zhang J, Zhang Z, Miller W, Lipman DJ (1997) Nucleic Acids Res 25:3389–3402
47. Thompson JD, Higgins DG, Gibson TJ (1994) Nucleic Acids Res 22:4673–4680
48. Schaumann T, Braun W, Wuthrich K (1990) Biopolymers 29:679–694
49. Laskowski RA, Rullmannn JA, MacArthur MW, Kaptein R, Thornton JM (1996) J Biomol NMR 8:477–486
50. Ito T, Deng X, Carr B, May WS (1997) J Biol Chem 272:11671–11673
51. Nguyen M, Millar DG, Yong VW, Korsmeyer SJ, Shore GC (1993) J Biol Chem 268:25265–25268
52. Blagosklonny MV (2001) Leukemia 15:869–874
53. Kern D, Volkman B, Luginbuhl P, Nohaile M, Kustu S, Wemmer D (1999) Nature 402:894–898
54. Volkman BF, Lipson D, Wemmer DE, Kern D (2001) Science 291:2429–2433
55. Nohaile M, Kern D, Wemmer D, Stedman K, Kustu S (1997) J Mol Biol 273:299–316
56. Chou J, Li H, Salvesen G, Yuan J, Wagner G (1999) Cell 96:615–624